







# Brazed carbon fiber fabric field emission cathode

Cite as: Rev. Sci. Instrum. **91**, 064702 (2020); <https://doi.org/10.1063/5.0006371>

Submitted: 02 March 2020 . Accepted: 17 May 2020 . Published Online: 05 June 2020

Brad W. Hoff , Sterling Beeson, David Simon , Wilkin Tang, Ronald Smith , Steven C. Exelby , Nicholas M. Jordan , Ali Sayir, Ronald M. Gilgenbach , P. David Lepell, and Tom Montoya



View Online



Export Citation



CrossMark

## ARTICLES YOU MAY BE INTERESTED IN

[Calibration and measurement performance analysis for a spectral band charge-coupled-device-based pyrometer](#)

Review of Scientific Instruments **91**, 064904 (2020); <https://doi.org/10.1063/1.5129758>

[A simple system for neutron diffraction at 4 K and elevated pressures](#)

Review of Scientific Instruments **91**, 063302 (2020); <https://doi.org/10.1063/5.0012508>

[A modified self-tuning fuzzy logic temperature controller for metal induction heating](#)

Review of Scientific Instruments **91**, 064905 (2020); <https://doi.org/10.1063/5.0006019>

**MCL**  
MAD CITY LABS INC.  
[www.madcitylabs.com](http://www.madcitylabs.com)

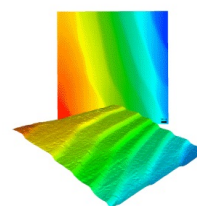
Nanopositioning  
Systems



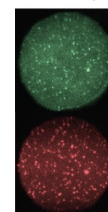
Modular  
Motion Control



AFM and NSOM  
Instruments



Single Molecule  
Microscopes



# Brazed carbon fiber fabric field emission cathode

Cite as: Rev. Sci. Instrum. 91, 064702 (2020); doi: 10.1063/5.0006371

Submitted: 2 March 2020 • Accepted: 17 May 2020 •

Published Online: 5 June 2020



Brad W. Hoff,<sup>1,a)</sup> Sterling Beeson,<sup>1</sup> David Simon,<sup>1</sup> Wilkin Tang,<sup>1</sup> Ronald Smith,<sup>2</sup> Steven C. Exelby,<sup>1,3</sup> Nicholas M. Jordan,<sup>3</sup> Ali Sayir,<sup>4</sup> Ronald M. Gilgenbach,<sup>3</sup> P. David Lepell,<sup>5</sup> and Tom Montoya<sup>6</sup>

## AFFILIATIONS

<sup>1</sup>Air Force Research Laboratory, Directed Energy Directorate, Kirtland AFB, New Mexico 87117, USA

<sup>2</sup>S-Bond Technologies, Harleysville, Pennsylvania 19438, USA

<sup>3</sup>Department of Nuclear Engineering and Radiological Sciences, University of Michigan, Ann Arbor, Michigan 48109, USA

<sup>4</sup>Air Force Office of Scientific Research, Arlington, Virginia 22203, USA

<sup>5</sup>Leidos, Albuquerque, New Mexico 87106, USA

<sup>6</sup>Voss Scientific, Albuquerque, New Mexico 87108, USA

<sup>a)</sup> Author to whom correspondence should be addressed: [brad.hoff@us.af.mil](mailto:brad.hoff@us.af.mil)

## ABSTRACT

Field emission cathodes, comprised of commercially available carbon fiber fabrics directly brazed to metal substrates, were fabricated and tested. Cathodes fabricated in this manner eliminate the need for an epoxy bond between the carbon fibers and the substrates and can be baked, in a vacuum, at high temperatures, limited by the re-melt temperature of the braze. Preliminary testing at mildly relativistic voltages (200 kV–300 kV) yielded average current emission densities of 100's of A/cm<sup>2</sup>, which are in line with previously published results on epoxy-bonded carbon fiber field emission cathodes.

<https://doi.org/10.1063/5.0006371>

## I. BACKGROUND

For applications requiring high current, high voltage electron beams, and long lifetime such as vacuum electron tubes and accelerators, field emission cathodes are typically used as the electron beam emitter. During field emission, the applied electric field is strong enough that electrons quantum mechanically tunnel through the potential barrier created at the surface of the cathode material by the process known as Fowler–Nordheim tunneling.<sup>1</sup> Field emission properties of a cathode are dependent on the strength of the applied electric field as well as the work function of the material, surface state, and electron transport properties within the material.

For vacuum electron devices, field emission cathodes based on carbon fiber emitters have emerged as a leading technology for generating high voltage, high current electron beams.<sup>2</sup> Some reasons for the selection of carbon fiber include its large surface area per unit volume, mechanical strength, flexibility, good resistance to erosion during electron emission in a vacuum, and operability over a wide range of temperature regimes.<sup>3</sup> In addition, carbon fiber field emission cathodes have been shown to operate into the space charge limited regime, as required for many vacuum electron tubes

and devices, achieving operation with relatively low outgassing,<sup>4</sup> at current densities reaching 100's of A/cm<sup>2</sup>.<sup>5–8</sup>

Carbon fiber field emission cathodes are typically fabricated with “carbon-on-epoxy” or “carbon-on-carbon” bonding methods,<sup>4,9</sup> in which a substrate material is first coated with a thin layer of adhesive or epoxy. Carbon fibers are then partially embedded in the adhesive layer using an electrostatic flocking process,<sup>10</sup> forming a random or semi-random array or “forest” of carbon fibers that are bonded to the substrate surface.<sup>2,4,9,11–13</sup> When the substrate material is a metal, a conductive epoxy is typically used, to ensure electrical conductivity between the substrate and the fibers<sup>4,9,14</sup> (the “carbon-on-epoxy” method). When the substrate material is bulk carbon, graphite, or some ceramics, a carbon bond may be formed by using an adhesive resin that can be chemically converted to a carbon or mostly carbon film by processing at high temperature<sup>9,15</sup> (the “carbon-on-carbon” method).

The primary goal of the present work was to explore the viability of field emission cathodes fabricated with an alternative carbon fiber bonding method that allows carbon fiber fabrics to be electrically and mechanically joined to the metal without the use of an epoxy layer. The selected process utilizes a carbon-wetting

brazing material<sup>16,17</sup> to form a conductive junction between the carbon fiber fabric and a copper or stainless steel substrate. By avoiding the use of the vacuum epoxy (and associated organic constituents of the epoxy) as a joining agent, carbon fiber cathodes can potentially be vacuum-baked at hotter temperatures (up to the braze re-melt temperature,  $<850^{\circ}\text{C}$ ) for longer periods of time to facilitate more effective removal of water and other adsorbed impurities.

## II. CATHODE CONSTRUCTION

### A. Cathode field emission material (carbon fabric)

Two commercially available carbon fiber fabrics, an “activated” carbon felt (ACF),<sup>18</sup> and a graphite felt electrode (GFE)<sup>19</sup> material were chosen as initial candidates for evaluation in the brazing process. The ACF fabric, having a thickness of  $\sim 3\text{ mm}$  and per-area density in the range of  $0.08\text{ g/cm}^3$ – $0.09\text{ g/cm}^3$ , was described by the manufacturer as being comprised of a mix of various types of carbon fibers that had been subjected to a high temperature ( $>600^{\circ}\text{C}$ ) steam treatment to increase fiber porosity (e.g., the “activation” process). The GFE fabric, having a thickness of  $\sim 2\text{ mm}$  and a density in the range of  $0.09\text{ g/cm}^3$ – $0.15\text{ g/cm}^3$ , was described by the manufacturer as being comprised of a graphitic carbon fiber derived from polyacrylonitrile (PAN).

Scanning electron microscopy (SEM) was performed on samples of both the ACF and GFE fabric. SEM images of the ACF fabric, showing selected areas of the sample at two different levels of magnification are provided in Figs. 1(a) and 1(b), respectively. SEM images of the GFE fabric, showing selected areas of the sample at two different levels of magnification are provided in Figs. 2(a) and 2(b), respectively.

Comparatively, the morphology and geometry of the fibers comprising the ACF and GFE fabrics were observed to be different from each other. The ACF fibers were  $\sim 10\text{ }\mu\text{m}$  in diameter with cylindrical cross sections and appeared to have rough surfaces. The GFE fibers appeared to be comprised of agglomerations of smaller  $\sim 2\text{ }\mu\text{m}$  diameter fibers. The cross sections of the agglomerated macro-fibers were irregular and appeared to range from  $\sim 8\text{ }\mu\text{m}$  to  $12\text{ }\mu\text{m}$ , depending on the fiber and viewing angle.

### B. Joining of the carbon fabric to the metal substrate

The brazing joining of graphite and carbides to various metals has been investigated back as far as the 1970s.<sup>20,21</sup> To wet and adhere non-reactive molten metals to graphite, this technique first requires metal plating layers on the graphite/carbon. In the 1990s, developments in reactive braze metal fillers permitted the application of “active” braze alloys made with small additions of active metals such as Ti, Hf, and/or Zr to braze ceramics and carbides without pre-plated layers on these carbon-based materials.<sup>20,22</sup> In 1998, further work was published that disclosed the use of active copper–silver based braze fillers with small additions of titanium to join graphite to metals.<sup>22</sup> The use of an “active” braze alloy to directly join the carbon fiber fabric layer to the metal substrate avoids the added complexity and potential contamination issues that would be introduced by a metal pre-plating step.

This past work in active brazing of graphite/carbon led to the selection of 32Cu–63Ag–1.75 w/o braze filler alloys to bond the

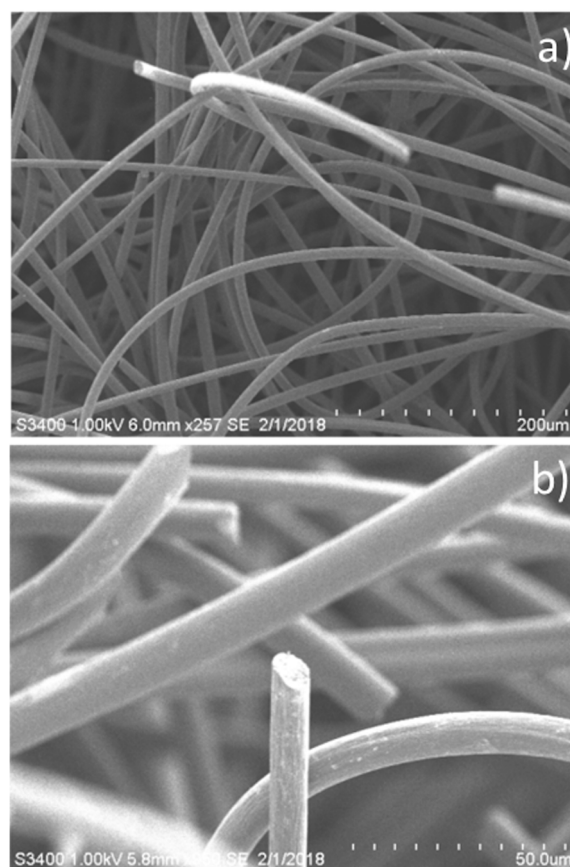


**FIG. 1.** (a) Scanning electron microscope image of the ACF fabric showing multiple constituent fibers. (b) Scanning electron microscope image of the end region of one of the individual fibers comprising the ACF fabric.

carbon fabrics to the copper and stainless steel bases of the cathode. The investigators specifically used the Cu–Ag–Ti braze paste (CuSil-ABA<sup>®</sup> from Morgan Advanced Materials) which consisted of prealloyed-325 mesh ( $45\text{ }\mu\text{m}$  nominal diameter) metal powder particles mixed with organic binders that would burn off completely without the production of free oxygen and decompose completely with no carbon residues below the filler metal melting temperatures of  $780^{\circ}\text{C}$ – $815^{\circ}\text{C}$ .

For this work, the copper and stainless steel base materials were immersed and/or wiped with lint-less fabrics to remove possible residual oils/greases prior to adding  $\sim 20\text{ }\mu\text{m}$  layers of the CuSil-ABA<sup>®</sup> paste to the metallic surfaces. The filler paste layer thickness was selected to minimize the infiltration of the carbon fabric with molten filler metals during the vacuum brazing cycle. After the pastes were evenly spread on their metallic bases, the carbon fabrics were lightly pressed against the applied paste layers on the base metals. After pressing the fabrics into the braze paste layers, the assemblies were dried at  $80^{\circ}\text{C}$  for 3 h–4 h to set the CuSil-ABA<sup>®</sup> paste binder and to drive off some of the volatile organics before the assembled parts were vacuum brazed.

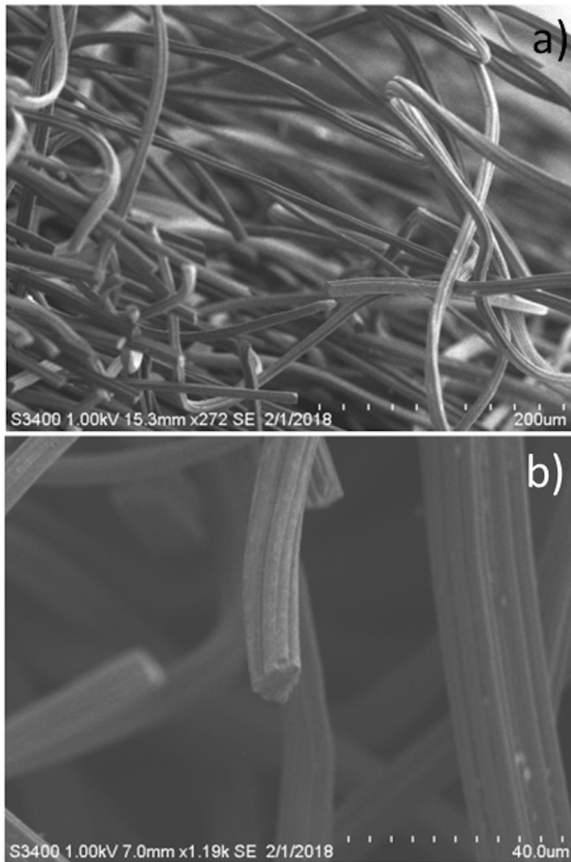


**FIG. 2.** (a) Scanning electron microscope image of the GFE fabric showing multiple constituent fibers. (b) Scanning electron microscope image of the end region of one of the individual fibers comprising the GFE fabric.

The assembled fabric/braze paste/metal paste parts were fixtured in the vacuum furnace with graphite flat or shaped tools in order to apply as uniform pressure on the fabric surfaces as possible. These tools were designed to achieve “dead loaded” pressures of  $1.0 \text{ g/mm}^2$  as the assemblies were brazed. In the braze cycle, the paste binder was decomposed and off-gassed, and the metal filler powder particles were subsequently melted such that the molten braze filler layer wetted the graphite/carbon fibers and the metal bases to achieve chemically reacting bonds. The vacuum braze cycle consisted of ramping from room temperature ( $\sim 25^\circ\text{C}$ ) to  $740^\circ\text{C}$ , maintaining pressures of  $1 \times 10^{-4}$  Torr or lower. Upon reaching the required temperature and vacuum pressure thresholds, the furnace is heated to the final braze temperature of  $860^\circ\text{C} \pm 10^\circ\text{C}$  for a 10 min hold. At the completion of the hold, the heater is de-energized and the furnace is allowed to cool to room temperature over multiple hours.

Initial test samples consisted of small 2.54 cm diameter stainless substrates with similarly sized patches of the ACF and GFE fabrics. Following successful joining [Fig. 3(a)], the ACF and GFE samples were then cross sectioned along a plane perpendicular to the surface of the samples, polished, and imaged under a microscope

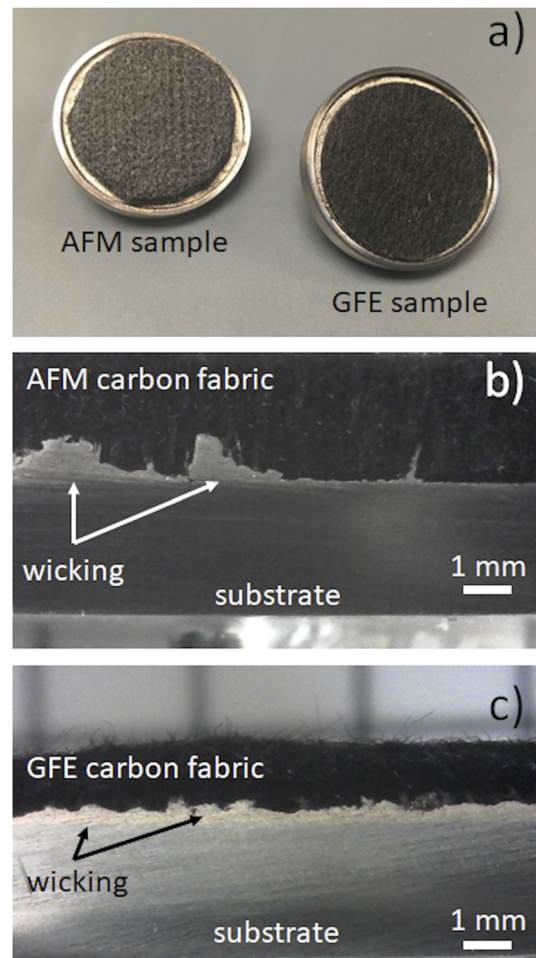


**FIG. 3.** (a) Test samples consisting of a 2.54 cm diameter stainless steel substrate joined to the ACF (left) and GFE (right) carbon fiber fabrics; (b) microscope image of a cross section of the ACF sample showing minor wicking at the braze interface; (c) microscope image of a cross section of the GFE sample showing minor wicking at the braze interface.

[Figs. 3(b) and 3(c), respectively]. Images of the samples showed that minor wicking of the braze had occurred during the joining process. Because the wicking regions remained well below the exposed surface of the fabric, the samples were, for the purposes of the present exploration, considered to be successfully joined, and the same joining process was utilized for a set of experimental cathodes intended for emission testing under high voltage.

### III. PROOF OF CONCEPT EXPERIMENTS: CROSSED-FIELD EMISSION

Experimental testing of two prototype cathodes in a crossed-field configuration, relevant to magnetrons, magnetically insulated line oscillators, and similar high power microwave (HPM) sources, was performed. Two cathodes (one each of the ACF and GFE fabrics) were fabricated for an existing recirculating planar crossed-field



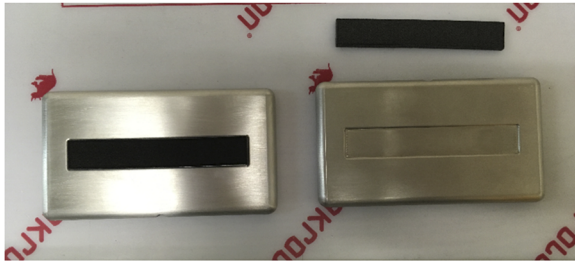


**FIG. 4.** Photo of stainless steel cathode substrates and carbon fiber fabrics (GFE left and ACF upper right) prior to brazing.

amplifier (RPCFA) experiment.<sup>23,24</sup> Each cathode consisted of a polished stainless steel block, approximately  $6.6 \times 12.0 \times 1.0 \text{ cm}^3$ , with a  $1.5 \times 9.1 \text{ cm}^2$  emission area ( $13.7 \text{ cm}^2$ ) on one side, as shown in Fig. 4. A fully detailed description of the experimental setup, procedure, and results for the RPCFA experiment is available in Ref. 24; however, key findings associated with the performance of the ACF and GFE brazed cathodes, referred to in Ref. 24 as “Cathode A” and “Cathode B,” respectively, are summarized hereinafter.

All crossed-field cathode testings were performed with a 1.5 cm anode to cathode gap and with a cathode voltage of  $\sim 300 \text{ kV}$ . Magnetic field values between 0.20 T and 0.25 T were used. During initial comparison testing of the brazed carbon fiber fabric cathodes, the ACF cathode was employed in 35 shots (with a “shot” being defined as a single pulsing of the Marx bank) and the GFE cathode was tested in 39 shots. These data were compared to a control set of 58 shots using an existing metal and Glyptal patterned cathode with the same cathode geometry.<sup>24</sup> In all cases, these shots had rise times of the order of 100 ns with pulse durations typically 200 ns–400 ns. Individual shots (pulses) were fired on a 2 min–5 min interval. Summary current data from these experiments are plotted in Fig. 5. Mean peak current is defined as the average over the dataset

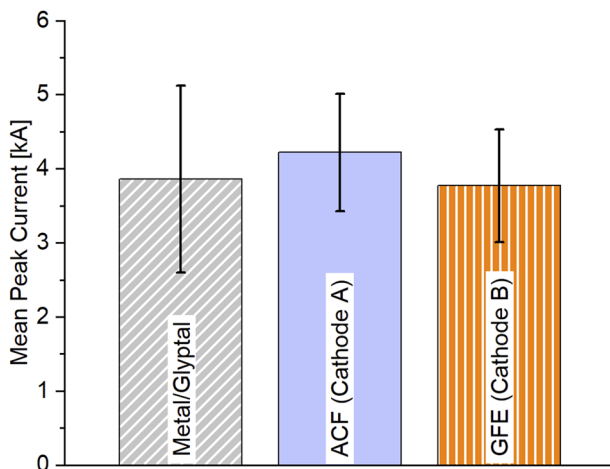


**FIG. 5.** Mean peak current emission for the metal/glyptal, ACF, and GFE cathodes tested in the RPCFA experiment. Error bars indicate one standard deviation from the mean.

of the peak current reached during the pulsed operation (shot) of the crossed-field amplifier. Current was measured by a Rogowski coil wound around the cathode stalk between the Marx bank and the cathode.

The ACF cathode was found to outperform the control cathode (metal/glyptal) by a statistically significant margin. The GFE cathode results were found to differ from those of the metal/glyptal cathode by a small, but statistically insignificant margin. Statistical significance was calculated based on a two-tailed, heteroscedastic, student's t-test using the metal/glyptal cathode as the control set. A threshold of 0.1 was used to determine statistical significance. Additionally, both the ACF and GFE cathodes significantly reduced the incidence of arcing (6% of shots for ACF and 5% of shots for GFE), as compared with the metal/glyptal cathode (17%). This is likely a result of lower outgassing from the carbon cathodes.

Calculating current density using the designed cathode emission area of  $13.7 \text{ cm}^2$  for the metal/glyptal, ACF, and GFE cathodes yields  $282 \text{ A/cm}^2$ ,  $308 \text{ A/cm}^2$ , and  $275 \text{ A/cm}^2$ , respectively. Even allowing for substantial emission from unintended portions of the cathode, emitted current densities are on par with the 100's of  $\text{A/cm}^2$  expected from carbon fiber field emission cathodes.<sup>6</sup>

#### IV. PROOF OF CONCEPT EXPERIMENTS: LINEAR BEAM EMISSION

Experimental testing of a brazed carbon fiber fabric cathode in a linear beam configuration was performed. The modulator used for experiments on the brazed carbon fiber cathode was the nonlinear transmission line (NLTL)-based electron beam driver described in Ref. 25. This modulator consists of a 15-stage Marx bank pulser, high power NLTL,<sup>26–28</sup> electron beam diode, and magnetized drift tube. The NLTL voltage diagnostics and drift tube electron beam diagnostics were configured in the same manner as that in previous experiments.<sup>25</sup>

The output waveform for the modulator, described in detail in Ref. 25, consists generally of a 20 ns–30 ns quasi-DC pulse with varying degrees of RF modulation (from a few 1's of % to 10's of %, depending on the NLTL bias setting). In place of the Friedman-style<sup>29</sup> cathode used in the original experiments,<sup>25</sup> an axially emitting annular electron beam cathode (Fig. 6) featuring the brazed

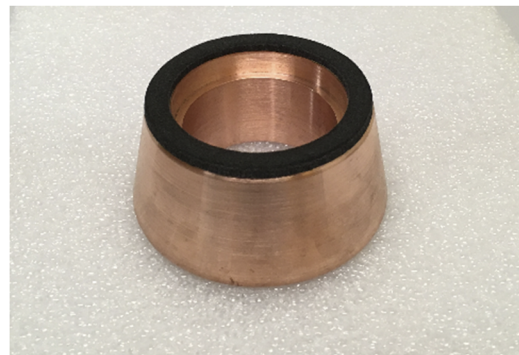


**FIG. 6.** Photo of the annular beam field emission cathode comprised of the ACF fabric (black annular layer) brazed to copper.

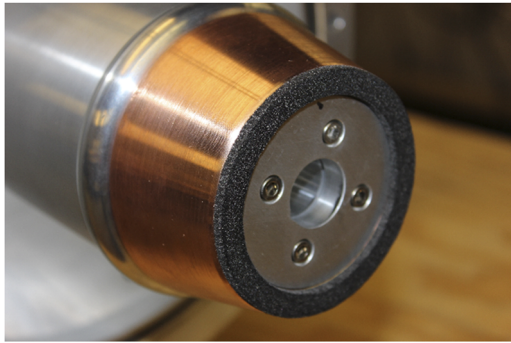


**FIG. 7.** Photo of the annular beam field emission cathode, comprised of an annular ACF fabric layer brazed to a tapered cylindrical copper substrate, mounted to the cathode stalk assembly.

ACF fabric field emission surface was used. A 2.70 cm radius center conductor, beginning 10.0 cm downstream from the cathode surface was included in the magnetized drift tube to increase electric field uniformity at the cathode surface and reduce space charge effects.

A brazed ACF cathode was used for the linear beam emission proof-of-concept experiments. The cathode's 16.03 cm<sup>2</sup> emission area consisted of an annular carbon fabric region with an inner radius of 2.79 cm and an outer radius of 3.59 cm, which was brazed to a tapered copper cylinder. A photo of the cathode after installation on the cathode stalk is shown in Fig. 7.

The initial beam emission experiments, using the brazed ACF carbon fiber fabric cathode, consisted of 81 shots across five different Marx charge voltages (10 kV, 15 kV, 20 kV, 25 kV, and 30 kV). Figure 8 provides a plot of mean peak current values vs peak voltage values for all shots performed at each Marx charge voltage. Error bars indicated one standard deviation from the mean. As was done for the Ref. 25 experiments, voltage was sampled using a D-dot at

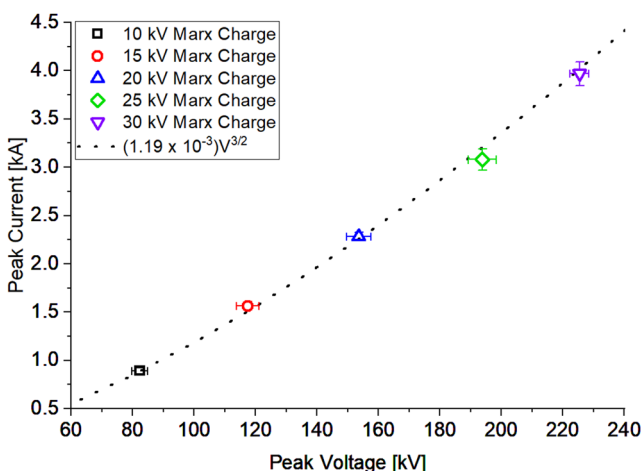


**FIG. 8.** Peak current values vs peak voltage values for cathode shots across five different Marx charge voltages (10 kV, 15 kV, 20 kV, 25 kV, and 30 kV).

the output end of the NLTL, and current was sampled with a B-dot 20 cm downstream of the cathode emission surface. Considering the calculated cathode emission area of 16.03 cm<sup>2</sup>, at the highest voltages, peak current density from the brazed carbon fabric cathode begins to approach values (100's of A/cm<sup>2</sup>) reported by others for carbon-on-carbon fiber cathodes with similar emission areas.<sup>7,8</sup> A V<sup>3/2</sup> dependence of current density on applied voltage indicates that the cathode operates in the space charge limited regime.<sup>30,31</sup>

## V. SUMMARY AND CONCLUSIONS

The authors have provided a preliminary exploration of the viability of field emission cathodes fabricated with an alternative carbon fiber bonding method (compared to typical "carbon-on-epoxy" or "carbon-on-carbon" bonds) that allows carbon fiber fabrics to be electrically and mechanically joined to the metal without the use of an epoxy layer. The selected process utilizes a carbon-wetting braze material to form a conductive junction between the carbon fiber fabric and a copper or stainless steel substrate. By avoiding the use of the vacuum epoxy (and associated organic constituents of the epoxy) as a joining agent, carbon fiber cathodes can potentially be vacuum-baked at hotter temperatures (up to the braze re-melt temperature) for longer periods of time to facilitate more effective removal of water and other adsorbed impurities.

Initial emission testing of brazed carbon fabric cathodes in crossed-field and linear beam configurations yielded current densities of 100's of A/cm<sup>2</sup> (exceeding 250 A/cm<sup>2</sup> at 230 kV). These current densities approach current density values described in the literature for carbon fiber field emission cathodes fabricated with carbon-on-epoxy and carbon-on-carbon techniques and having similar emission areas. The presence of the braze interface does not appear to substantially interfere with the transfer of current from the substrate to the carbon fiber electron emission layer. It has been shown by Zhang *et al.* that, with sufficient data, it is possible to characterize the contribution of the contact resistance at the interface layer between the emitter and the substrate.<sup>32</sup> Although the present datasets, being for the purposes of demonstrating proof-of-concept only, are not sufficient to adequately support such an analysis, this is of interest to the authors in the future characterization efforts.

It is known that for carbon-fiber-based field emitters described in the literature, the fiber geometry, fiber composition, and presence of coatings, such as CsI,<sup>2,12,33</sup> substantially impact cathode performance and emission uniformity. Thus, it is reasonable to expect that an exploration of other commercial or custom carbon fabrics with different fiber compositions could yield materials with superior field emission properties to the two materials evaluated in the present study. Additionally, coatings used on published carbon fiber cathodes, such as those described by Shiffler *et al.*,<sup>2,12,33</sup> would be expected to be compatible with a variety of carbon fiber fabrics and could potentially provide enhanced performance, compared to the uncoated carbon fabric.

## SUPPLEMENTARY MATERIAL

See the [supplementary material](#) for current data supporting Fig. 5 and current vs voltage data supporting Fig. 8.

## ACKNOWLEDGMENTS

This work was funded, in part, by the Air Force Research Laboratory. B. Hoff and D. Simon were funded, in part, by Air Force Office of Scientific Research LRIR Grant No. FA9550-19RDCOR025. W. Tang and B. Hoff were funded, in part, by Air Force Office of Scientific Research LRIR Grant No. FA9550-20RDCOR018. S. Exelby, N. Jordan, and R. Gilgenbach were funded by Air Force Office of Scientific Research Grant No. FA9550-15-1-0097. The braze development was done at S-Bond Technologies by M. Shaw and J. Conroy.

## DATA AVAILABILITY

The data that support the findings of this study are available from the corresponding author upon reasonable request.

## REFERENCES

- <sup>1</sup>R. H. Fowler and L. Nordheim, *Proc. R. Soc. London, Ser. A* **119**, 173 (1928).
- <sup>2</sup>D. Shiffler, M. Ruebush, M. Haworth, R. Umstattd, M. LaCour, K. Golby, D. Zagar, and T. Knowles, *Rev. Sci. Instrum.* **73**, 4358 (2002).
- <sup>3</sup>W. Tang, K. Golby, M. Lacour, and T. Knowles, *IEEE Trans. Plasma Sci.* **42**, 2580 (2014).
- <sup>4</sup>C. A. Schlise, *Explosive Emission Cathodes for High Power Microwave Devices: Gas Evolution Studies* (Naval Postgraduate School, 2004).
- <sup>5</sup>W. Tang, D. Shiffler, K. Golby, M. LaCour, and T. Knowles, *J. Vac. Sci. Technol., B: Nanotechnol. Microelectron.: Mater., Process., Meas., Phenom.* **32**, 052202 (2014).
- <sup>6</sup>J. Benford, J. A. Swegle, and E. Schamiloglu, *High Power Microwaves*, 3rd. (CRC Press, Boca Raton, FL, 2016).
- <sup>7</sup>J. M. Parson, C. F. Lynn, J. J. Mankowski, A. A. Neuber, and J. C. Dickens, *IEEE Trans. Plasma Sci.* **42**, 3982 (2014).
- <sup>8</sup>C. Lynn, J. Walter, A. Neuber, J. Dickens, and M. Kristiansen, in *Proceedings of 2012 IEEE International Power Modulator and High Voltage Conference (IPMHVC 2012)* (IEEE, 2012), pp. 772–775.
- <sup>9</sup>T. R. Knowles, in *NRL Workshop on Cathodes Relativistic Electron Beams* (U.S. Naval Research Laboratory, Washington, DC, 2001), pp. 1–13.
- <sup>10</sup>Y. Sekii and T. Hayashi, *IEEE Trans. Dielectr. Electr. Insul.* **16**, 649 (2009).
- <sup>11</sup>D. Shiffler, M. LaCour, K. Golby, M. Sena, M. Mithcell, M. Haworth, K. Hendricks, and T. Spencer, *IEEE Trans. Plasma Sci.* **29**, 445 (2001).
- <sup>12</sup>D. A. Shiffler, U.S. patent 6,683,399 (27 January 2004).
- <sup>13</sup>D. Shiffler, J. Heggemeier, M. LaCour, K. Golby, and M. Ruebush, *Phys. Plasmas* **11**, 1680 (2004).
- <sup>14</sup>T. R. Knowles and C. L. Seaman, U.S. patent 7,132,161 (7 November 2006).
- <sup>15</sup>Y. Yamada and D. D. L. Chung, *Carbon* **46**, 1798 (2008).
- <sup>16</sup>S-Bond Technologies, *S-Bond® Joining Graphite and Carbon to Metals* (S-Bond Technologies, Lansdale, PA, 2009).
- <sup>17</sup>R. W. Smith, U.S. patent 6,047,876 (11 April 2000).
- <sup>18</sup>See [www.Ceramaterials.Com](http://www.Ceramaterials.Com) for CeraMaterials, Activated Carbon Felt, Port Jervis, NY, n.d..
- <sup>19</sup>CeraMaterials, 1 (n.d.).
- <sup>20</sup>American Welding Society, *Brazing Handbook*, 5th ed. (American Welding Society, Miami, FL, 2007).
- <sup>21</sup>I. Amato, P. G. Cappelli, and P. C. Martinengo, *Weld. J.* **53**, 623 (1974).
- <sup>22</sup>T. Oyama and H. Mizuhara, *Weld. World* **41**, 412 (1998).
- <sup>23</sup>S. C. Exelby, G. B. Greening, N. M. Jordan, D. A. Packard, D. Simon, Y. Y. Lau, B. W. Hoff, and R. M. Gilgenbach, *IEEE Trans. Electron Devices* **65**, 2361 (2018).
- <sup>24</sup>S. C. Exelby, *Recirculating Planar Crossed-Field Amplifiers* (University of Michigan, 2019).
- <sup>25</sup>B. W. Hoff, D. M. French, D. S. Simon, P. D. Lepell, T. Montoya, and S. L. Heidger, *Phys. Rev. Accel. Beams* **20**, 100401 (2017).
- <sup>26</sup>D. M. French and B. W. Hoff, *IEEE Trans. Plasma Sci.* **42**, 3387 (2014).
- <sup>27</sup>J. Schrock, P. D. Lepell, J. Gilbrech, H. Wood, R. Richter-Sand, B. Hoff, and S. Heidger, in *2018 IEEE International Power Modulator and High Voltage Conference* (IEEE, Jackson Lake, WY, 2018).
- <sup>28</sup>J. A. Schrock, B. W. Hoff, D. H. Simon, S. L. Heidger, P. Lepell, J. Gilbrech, H. Wood, and R. Richter-Sand, *IEEE Trans. Dielectr. Electr. Insul.* **26**, 412 (2019).
- <sup>29</sup>M. Friedman, J. Krall, Y. Y. Lau, and V. Serlin, *J. Appl. Phys.* **64**, 3353 (1988).
- <sup>30</sup>C. D. Child, *Phys. Rev. (Series I)* **32**, 492 (1911).
- <sup>31</sup>I. Langmuir, *Phys. Rev.* **2**, 450 (1913).
- <sup>32</sup>P. Zhang, S. B. Fairchild, T. C. Back, and Y. Luo, *AIP Adv.* **7**, 125203 (2017).
- <sup>33</sup>D. Shiffler, M. Haworth, K. Cartwright, R. Umstattd, M. Ruebush, S. Heidger, M. LaCour, K. Golby, D. Sullivan, P. Duselis, and J. Luginsland, *IEEE Trans. Plasma Sci.* **36**, 718 (2008).